Chen et al. Journal of Neuroinflammation (2016) 13:204
DOI 10.1186/s12974-016-0661-0

Journal of Neuroinflammation

RESEARCH Open Access

The glucagon-like peptide-1 receptor agonist exendin-4 ameliorates warfarin-associated hemorrhagic transformation after cerebral ischemia

Fangzhe Chen[1†], Weifeng Wang[2†], Hongyan Ding[1], Qi Yang[1], Qiang Dong[1*] and Mei Cui[1*]

Abstract

Background: As the number of patients with cardioembolic ischemic stroke is predicted to be double by 2030, increased burden of warfarin-associated hemorrhagic transformation (HT) after cerebral ischemia is an expected consequence. However, thus far, no effective treatment strategy is available for HT prevention in routine clinical practice. While the glucagon-like peptide-1 receptor (GLP-1R) agonist exendin-4 (Ex-4) is known to protect against oxidative stress and neuronal cell death caused by ischemic brain damage, its effect on preventing warfarin-associated HT after cerebral ischemia is yet unknown. Therefore, we hypothesized that Ex-4 would stabilize the blood-brain barrier (BBB) and suppress neuroinflammation through PI3K-Akt-induced inhibition of glycogen synthase kinase-3β (GSK-3β) after warfarin-associated HT post-cerebral ischemia.

Methods: We used male C57BL/6 mice for all experiments. A 5-mg warfarin sodium tablet was dissolved in animals' drinking water (effective warfarin uptake 0.04 mg (2 mg/kg) per mouse). The mice were fed for 0, 6, 12, and 24 h with ad libitum access to the treated water. To study the effects of Ex-4, temporary middle cerebral artery occlusion (MCAO) was performed. Then, either Ex-4 (10 mg/kg) or saline was injected through the tail vein, and in the Ex-4 + wortmannin group, PI3K inhibitor wortmannin was intravenously injected, after reperfusion. The infarct volume, neurological deficits, and integrity of the BBB were assessed 72 h post MCAO. One- or two-way ANOVA was used to test the difference between means followed by Newman–Keuls post hoc testing for pair-wise comparison.

Results: We observed that Ex-4 ameliorated warfarin-associated HT and preserved the integrity of the BBB after cerebral ischemia through the PI3K/Akt/GSK-3β pathway. Furthermore, Ex-4 suppressed oxidative DNA damage and lipid peroxidation, attenuated pro-inflammatory cytokine expression levels, and suppressed microglial activation and neutrophil infiltration in warfarin-associated HT post-cerebral ischemia. However, these effects were totally abolished in the mice treated with Ex-4 + the PI3K inhibitor—wortmannin. The PI3K/Akt-GSK-3β signaling pathway appeared to contribute to the protection afforded by Ex-4 in the warfarin-associated HT model.

Conclusions: GLP-1 administration could reduce warfarin-associated HT in mice. This beneficial effect of GLP-1 is associated with attenuating neuroinflammation and BBB disruption by inactivating GSK-3β through the PI3K/Akt pathway.

Keywords: Cerebral ischemia, Exendin-4, Hemorrhagic transformation, Blood-brain barrier, Neuroinflammation, PI3K/Akt-GSK-3β signaling pathway, Warfarin

(Continued on next page)

* Correspondence: dong_qiang@fudan.edu.cn; cuimei@fudan.edu.cn
†Equal contributors
[1]Department of Neurology, Huashan Hospital, State Key Laboratory of Medical Neurobiology, Fudan University, No. 12 Middle Wulumuqi Road, Shanghai 200040, China
Full list of author information is available at the end of the article

(Continued from previous page)

Abbreviations: 8-OHdG, 8-hydroxy-2′-deoxyguanosine; AF, Atrial fibrillation; BBB, Blood-brain barrier; Ex-4, Exendin-4; GLP-1R, Glucagon-like peptide-1 receptor; GSK-3β, Glycogen synthase kinase-3β; HHE, 4-hydroxyhexenal; HT, Hemorrhagic transformation; ICAM-1, Interstitial cell adhesion molecule-1; IL-1β, Interleukin-1 beta; INR, International normalized ratio; MCAO, Middle cerebral artery occlusion; PBS, Phosphate-buffered saline; PI3K, Phosphatidylinositol 3- kinase; RIPA, Radioimmunoprecipitation assay buffer; TNF-α, Tumor necrosis factor-α; TTC, 2,3,5-triphenyltetrazolium chloride; VCAM-1, Vascular cell adhesion molecule-1

Background

Globally, ischemic stroke is one of the leading causes of death and long-term disability [1]. The number of patients with cardioembolic ischemic stroke resulting from nonvalvular atrial fibrillation (AF), the major cause of cardioembolic ischemic stroke, is predicted to double by 2030 [2, 3]. Consequently, a growing burden of warfarin-associated hemorrhagic transformation (HT) after cerebral ischemia can be expected [4–6].

Early HT can occur as a complication of cardioembolic ischemic stroke [7]. Additionally, a higher rate of hematoma expansion and a worse clinical outcome have been reported in warfarin-associated HT patients [8–10]. However, no effective treatment strategy is available for prevention of HT in clinical practice. Experimental studies of cerebral ischemia have established increase in the permeability of the blood-brain barrier (BBB) after ischemia/reperfusion injury as one of the major causes of HT [11, 12].

The glucagon-like peptide-1 receptor (GLP-1R) agonist exendin-4 (Ex-4) is a long-acting analog of the endogenous insulinotropic peptide GLP-1. Both GLP-1 and Ex-4 have multiple physiologic functions, such as the induction of glucose-dependent insulin release, inhibition of glucagon secretion, stimulation of B cell replication, and antiapoptotic action [13]. Owing to their small molecule size, both GLP-1 and Ex-4 can diffuse across the BBB in the central nervous system and provide neuroprotection in cerebral ischemia [14, 15]. While it has been reported that Ex-4 can protect against oxidative products and neuronal cell death caused by ischemic brain damage, it is yet unknown whether Ex-4 is effective in preventing warfarin-associated HT after cerebral ischemia.

Previous studies have shown that after a hemorrhagic stroke, cytotoxic events activate the ubiquitously expressed glycogen synthase kinase-3β (GSK-3β), which increases the expression of β-catenin [16, 17] and subsequently decreases the expressions of claudins [18]. There is substantial evidence that GSK-3β inhibition (tyrosine-216 dephosphorylation) reduces neuronal apoptosis [19–21] and attenuates neuroinflammation in neurodegenerative models [22–24]. Pharmacological stimulation of GLP-1R activates the phosphatidylinositol 3-kinase (PI3K)-Akt signaling pathway, and a number of studies have linked GSK-3β with the PI3K/Akt pathway, thereby showing that phosphorylated Akt inactivates GSK-3β via tyrosine-216 dephosphorylation. Herein, we hypothesized that Ex-4 would stabilize the BBB and suppress neuroinflammation through PI3K-Akt-induced inhibition of GSK-3β after warfarin-associated HT post-cerebral ischemia in mice.

Methods

Animals

All experiments were conducted using male C57BL/6 mice (body weight 18–25 g) at a constant temperature and with a consistent light cycle (from 07:00 to 18:00) under normal diet. This study was carried out in accordance with the Guide for the National Science Council of the Republic of China. All animals were treated according to protocols approved by the Institutional Animal Care and Use Committee of Fudan University.

A 5-mg warfarin sodium tablet (Coumadin™, Sigma-Aldrich, St. Louis, MO, USA) was dissolved in 375 mL of water. The C57 BL/6 mice were fed for 0, 6, 12, and 24 hours with ad libitum access to the treated water. Assuming a mouse body weight of 20 g and a water consumption rate of 15 mL/100 g per 24 h, this dosage corresponds to a warfarin uptake of 0.04 mg (2 mg/kg) per mouse over a 24-h period. Similar doses of warfarin have been previously used [25]. After 24 h, the warfarin was withdrawn and middle cerebral artery occlusion was performed (Additional file 1: Figure S1). For the international normalized ratio (INR) measurement, the mice were under deep anesthesia, a peritoneal midline incision was performed, and 0.6 mL blood was drawn from the inferior caval vein as previously described [26]. Blood was transferred to glass tubes (BD Vacutainer®) containing sodium citrate as the anticoagulant. Measurements of INR values and prothrombin time were performed in the Department of Central Laboratory, Jingan District Centre Hospital, Shanghai, China.

Temporary middle cerebral artery occlusion and drug treatment

Mice were anesthetized with ketamine/xylazine (65/6 mg/kg, i.p), and their body temperature was maintained at 37 °C by a heating pad and feedback control system (FHC, Bowdoin, ME, USA). A laser Doppler probe was fixed on the skull 5 mm lateral and 2 mm posterior to the bregma.

A coated filament was placed on the right middle cerebral artery (MCA) with concurrent recording of laser Doppler cerebral blood flow to ensure that the cerebral blood flow decreased to below 25 % of the baseline. After 45 min, the filament was removed (Additional file 2: Figure S2). Either Ex-4 (10 mg/kg) or saline was injected through the tail vein immediately after reperfusion. In the Ex-4 + wortmannin group, we intravenously injected 15 μL/kg wortmannin (Sigma-Aldrich), a non-specific, covalent inhibitor of PI3K immediately after reperfusion.

Assessment of infarct volume, neurological deficits, and blood-brain barrier

All the mice were killed 72 h after temporary middle cerebral artery occlusion (MCAO), and brain tissues were incubated in 2,3,5-triphenyltetrazolium chloride (TTC) for 1 h. The infarct area in each slice was analyzed by a computerized image analysis system, and the infarct volume was calculated by multiplying the distance between sections [27]. Neurological score was determined 72 h after MCAO, according to the graded scoring system described previously by Li et al. [28]. Assessment of motor coordination deficits was performed on days 3 and 7 using the rota rod as previously described [29]. Investigators who performed MCAO models, evaluation of infarct volumes, neurological scales, and rota rod were blinded to all the experimental protocols and drug treatments. To measure BBB permeability, Evans blue (Sigma-Aldrich) was dissolved in saline (2 %) and injected into the right jugular vein 72 h after MCAO. The animals were then killed, and the brain hemispheres were homogenized in 3 mL of *N*,*N*-dimethylformamide (Sigma-Aldrich); incubated for 18 h at 55 °C; and centrifuged. The supernatants were subjected to spectrophotometry at 620 nm.

Quantification of hemorrhagic transformation

The hemoglobin content in brain tissue was quantified by spectrophotometric assay. The hemispheric brain tissue was homogenized with phosphate-buffered saline (PBS) and centrifuged at 13,000×*g* for 30 min. The hemoglobin-containing supernatant was collected, 80 μL of Drabkin reagent (Sigma) was added to 20-μL supernatant aliquots, and the sample was kept standing for 15 min at room temperature. The optical density in each group was measured at 540 nm, and hemorrhage volume was expressed in equivalent units by comparison with a reference curve generated using homologous blood.

Western blotting

Striatal brain tissues from the MCA were lysed with radioimmunoprecipitation assay buffer (RIPA) containing protease inhibitors (Sigma-Aldrich, St. Louis, MO, USA). Proteins were separated by SDS-PAGE and then transferred onto a nitrocellulose membrane. The membranes were incubated overnight at 4 °C with the following primary antibodies: anti-p-GSK-3β (Tyr216, 1:1000, Abcam Inc., Cambridge, MA); anti-GSK-3β (1:1000, Abcam); anti-β-actin (1:5000, Sigma-Aldrich); anti-p-β-catenin (Ser33/37/Thr41, 1:2000, Cell Signaling Technology Inc., Danvers, MA); anti-β-catenin (1:1000, Abcam), anti-claudin-3 (1:2000, Santa Cruz, CA); anti-claudin-5 (1:2000, Santa Cruz); anti-p-Akt (Ser473, 1:2000, Cell Signaling); anti-Akt (1:2000, Cell Signaling); anti-ICAM-1 (1:1000, Abcam); anti-VCAM-1 (1:1000, Abcam); anti-IKK-β (1:2000, Santa Cruz); anti-NF-kB (1:2000, Santa Cruz); anti-HHE (1:1,000, Abcam); anti-Iba1 (1:1,000, Abcam); and anti-myeloperoxidase (MPO) (1:2000, Santa Cruz). Secondary antibodies conjugated with horseradish peroxidase were used, and immunoreactivity was visualized by chemiluminescence (Super-Signal Ultra, Pierce, Rockford, IL, USA). Bands of interest were analyzed and quantified using Scion Image.

siRNA-mediated GSK-3β gene knockdown

The small interfering RNA (siRNA)-mediated GSK-3β gene knockdown was performed as previously described [30]. Briefly, two pairs of GSK-3β siRNAs (21500 R12-1717, R12-1719; Cell Signaling) with a total volume of 4 μL (2 μL each) were stereotaxically injected to the right lateral ventricle following coordinates relative to the bregma: AP = −0.4 mm, L = −1.0 mm, and H = − 2.0 mm (from the brain surface) 48 h prior to MCAO.

Measurement of cytokine concentration

Striatal brain tissues from the MCA were homogenized and collected by centrifugation at 15,000×*g* for 30 min at 4 °C and then stored at −70 °C until the assay was performed. The supernatant was assayed for tumor necrosis factor-α (TNF-α) and interleukin-1 beta (IL-1β) using enzyme-linked immunosorbent assays (ELISA; R&D Biosystems) as described previously [31].

Measurement of 8-OHdG formation in the brain

Concentration of 8-hydroxy-2′-deoxyguanosine (8-OHdG) in brain DNA was measured by Piao et al.'s method [32], with slight modifications. Briefly, 200 mg of brain tissue was homogenized in 0.25 M sucrose solution. DNA was extracted from the homogenate under anaerobic conditions. The 8-OHdG content in the brain was measured by using an HPLC-ECD as previously described [33]. Each brain sample was examined in duplicate.

Immunohistochemistry

Seventy-two hours after MCAO, the mice were anesthetized and first perfused with saline followed by fixation with buffered paraformaldehyde (4 %). The brains were removed and post-fixed in 4 % paraformaldehyde; the

paraformaldehyde was then removed and replaced with 30 % sucrose solution overnight. Then 15-μm coronal sections were obtained on a cryostat. The slices were blocked with PBS containing 5 % bovine serum albumin (BSA), 10 % goat serum, and 0.3 % Triton-X 100. Next, the slices were incubated with the primary antibodies anti-Iba1 (1:250, Abcam) and anti-TNF-α (1:100, Santa Cruz) overnight at 4 °C. Then Alexa Fluor 488 or 595 labeled secondary antibody (Molecular Probes Inc., Eugene, OR, USA) for 2 h at room temperature. The tissue sections were washed twice in PBS and then immersed in DAPI (Molecular Probes) solution (1:1000 dilution) for 10 min. The sections were finally rinsed in distilled water and fixed with a coverslip with anti-fade mounting medium.

Assessment of microglia activation

First, microglia activation were counted and morphologically characterized based on the following criteria. Cells with an oval cell body containing a small volume of cytoplasm and long, thin, delicate, and radially branched processes were classified as ramified microglia [34]. Activated microglia were defined as having an enlarged soma (width greater or equal to 30 μm) and a broad-flattened appearance with the common presence of several lamellapodia [35]. This morphological classification was then confirmed by using a methodology of semi-automatic image analysis to analyze the cell body to cell size ratio in Iba1-stained brain sections as described before [36] by ImageJ software.

Statistical analysis

All values are expressed as mean ± standard deviation (SD). Differences between means were analyzed using either one-way or two-way ANOVA followed by Newman–Keuls post hoc testing for pair-wise comparison using SigmaStat v 3.5®. A P value <0.05 was considered statistically significant.

Results

Exendin-4 ameliorated warfarin-associated HT after cerebral ischemia

To examine the influence of warfarin on animal PT-INR values, the mice were killed at the indicated time points and the PT-INR values were measured. After warfarin administration, the PT-INR values increased in a time-dependent manner (Fig. 1a). After 24 h of warfarin administration, PT-INR values were elevated (mean = 3.85 ± 1.12; $n = 6$) and reached the therapeutic span used in humans. These results were consistent with those previously reported [26]. In view of these results, we decided to use 24 h as the warfarin administration time for all subsequent experiments.

MCAO induced a sharp drop of rCBF, leading to extensive infarction in the cerebral cortical and subcortical areas over a series of brain sections in the mice (Fig. 1b, d). Compared with the MCAO+/Ex-4 group, warfarin treatment did not increase the infarct size or neurological deficits. However, warfarin significantly exacerbated HT after cerebral ischemia. Ex-4 suppressed this exacerbation (Fig. 2a). Moreover, Ex-4 showed striking protective effects to reduce to infarct volume and improve neurological function in MCAO mice with or without warfarin treatment (Fig. 1c–f).

Exendin-4 preserves the BBB integrity in warfarin-associated HT after cerebral ischemia

Functional barrier properties were evaluated using Evans blue assays, 72 h after surgery. Significantly more extravasated dye was measured in the ischemic hemispheres of mice subjected to warfarin treatment compared with the control group. Ex-4 preserved BBB integrity in the model of warfarin-associated HT after MCAO, which was associated with significantly reduced dye extravasation in Ex-4-treated animals (Fig. 2b).

Claudin-3 and claudin-5 are transmembrane proteins essential for maintaining the diffusion barrier provided by tight junctions [37, 38]. Previous studies reported the regulatory role of activation of GSK-3β and β-catenin in claudin-3 and claudin-5 gene expression, respectively [39]. Western blot analyses of the ischemic brain were conducted at 72 h after MCAO. Changes in protein expression of phosphorylated and, therefore, activated GSK-3β (p-GSK-3β, Tyr216) were quantified as a ratio to total GSK-3β (Fig. 3a, b). GSK-3 phosphorylation was significantly increased in the warfarin-treated mice compared with the control group. However, Ex-4 significantly reduced the p-GSK-3β/GSK-3β ratio. Consistent with these results, increased phosphorylated β-catenin levels were also found in warfarin-treated mice compared with the control group (Fig. 3c, d). Ex-4 significantly reduced the p-β-catenin/β-catenin ratio. Tight junction protein expressions were also detected. As shown in Fig. 3e–h, claudin-3 and claudin-5 levels were reduced in the model of warfarin-associated HT after MCAO compared with MCAO mice. However, Ex-4 treatment significantly reversed the reduction.

Exendin-4 ameliorated warfarin-associated HT after cerebral ischemia through PI3K/Akt/GSK-3β pathway

It has been reported that activated Akt (p-Akt) can inactivate GSK-3β and reduce the amount of GSK-3β available for phosphorylation (through the tyrosine-216 form) [40, 41]. The inactivation of GSK-3β, specifically through tyrosine-216 dephosphorylation, increased β-catenin, which is an important factor in maintaining BBB integrity [42, 43].

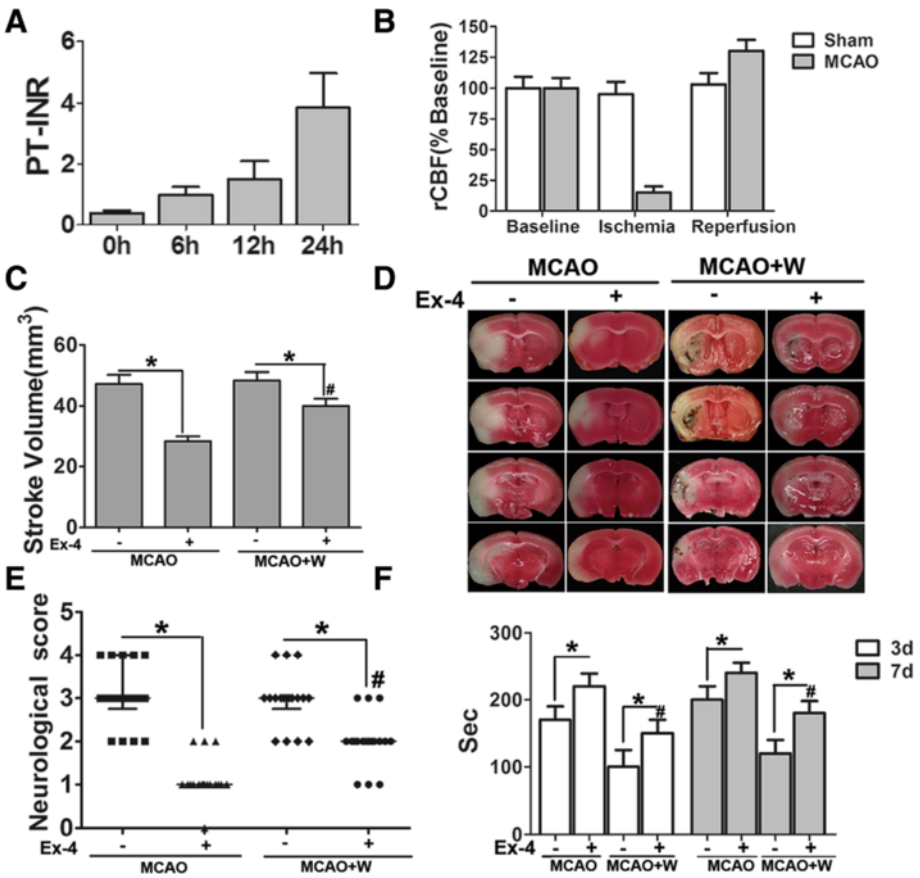

Fig. 1 Exendin-4 treatment reduced the stroke volume and improved neurological function after cerebral ischemia. **a** Prothrombin time-international normalized ratio values (PT-INR) in non-MCAO mice after 0, 6, 12, and 24 h of warfarin administration through drinking water. **b** Regional cerebral blood flow (rCBF) in both ischemic and reperfusion stages was recorded using laser Doppler cerebral blood flow. **c** Exendin-4 (Ex-4, 10 mg/kg) was injected through the tail vein immediately after reperfusion. The infarct volume was measured 72 h after middle cerebral artery occlusion (MCAO) using TTC straining. **d** Representative images of TTC straining showing the ischemic area and hemorrhage transformation. **e**, **f** Exendin-4 (Ex-4, 10 mg/kg) was injected through tail vein immediately after reperfusion. The neurological deficits were measured 72 h after MCAO, and assessment of motor function was analyzed on days 3 and 7 using rota rod after MCAO. Data are presented as mean ± SD and analyzed by two-way ANOVA. $^{*}P < 0.05$ compared with the Ex-4(–) group, $^{\#}P < 0.05$ compared with the MCAO+/Ex-4(+) group

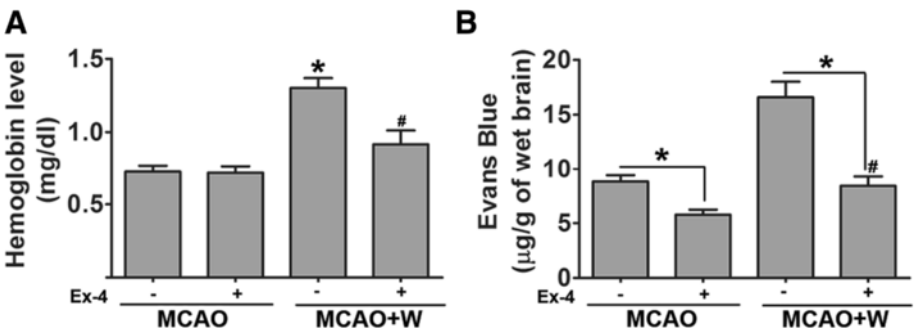

Fig. 2 Exendin-4 treatment reduced warfarin-associated HT after cerebral ischemia. **a** Brain hemoglobin levels were evaluated at 72 h after middle cerebral artery occlusion (MCAO). Data are presented as mean ± SD and analyzed by two-way ANOVA. $^{*}P < 0.05$ compared with the MCAO+/Ex-4(–) group, $^{\#}P < 0.05$ compared with the MCAO+/Ex-4(+) group. **b** Blood-brain barrier (BBB) integrity in MCAO mice were assessed after Evans blue staining. Data are presented as mean ± SD and analyzed by two-way ANOVA. $^{*}P < 0.05$ compared with the Ex-4(–) group, $^{\#}P < 0.05$ compared with the MCAO+/Ex-4(+) group

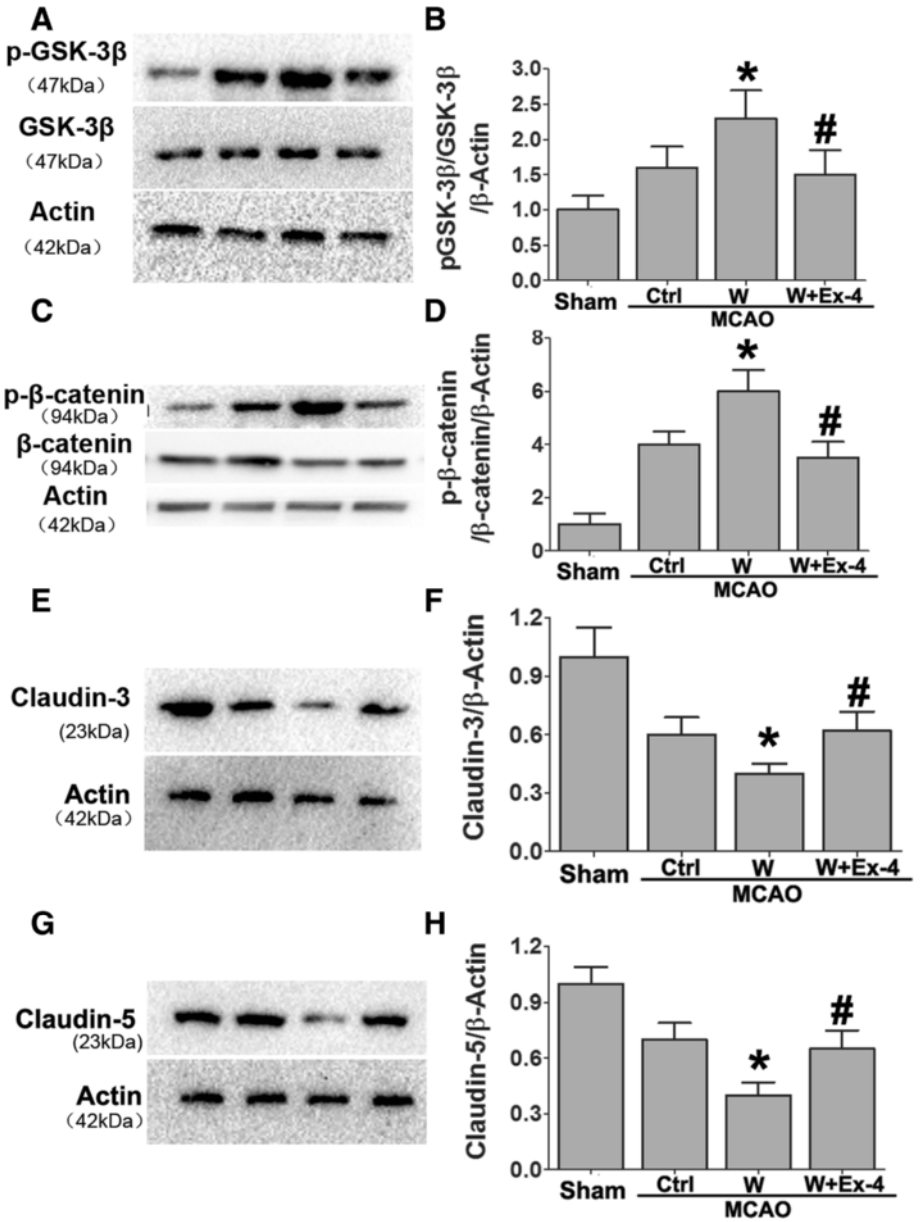

Fig. 3 Exendin-4 treatment preserved BBB integrity in warfarin-associated HT after cerebral ischemia. Western blot analysis of **a**, **b** p-GSK-3β/GSK-3β; **c**, **d** p-β-catenin/β-catenin; **e**, **f** claudin-3; and **g**, **h** claudin-5. Representative blots from six independent experiments with similar results are shown. (*Sham*: sham-operated group, *Ctrl*: MCAO group, *W*: warfarin-associated HT group, *W + Ex-4*: warfarin-associated HT pretreatment with Ex-4). Data are presented as mean ± SD from six independent experiments and analyzed by one-way ANOVA. $^{*}P < 0.05$ vs. MCAO group; $^{\#}P < 0.05$ compared with warfarin-associated HT group

To examine if warfarin and Ex-4 could phosphorylate Akt after cerebral ischemia, the phosphorylation of Akt was examined 72 h after MCAO. After normalizing the values of the active p-Akt with the amount of total Akt (Akt) in each sample, we observed an increase in the Ex-4-treated mice compared to warfarin treatment alone. We indirectly studied the activation of Akt by measuring the phosphorylation of its downstream target GSK-3β in the same brain areas. As compared with the warfarin-treated MCAO mice, Ex-4 treatment significantly suppressed the phosphorylation of GSK-3β. These phosphorylation changes of Akt and GSK-3β were totally abolished when the mice were treated with Ex-4 in combination with the PI3K inhibitor—wortmannin (Fig. 4).

These results showed that Ex-4 induced PI3K/Akt pathway activation and subsequent GSK-3β inactivation in the model of warfarin-associated HT after cerebral

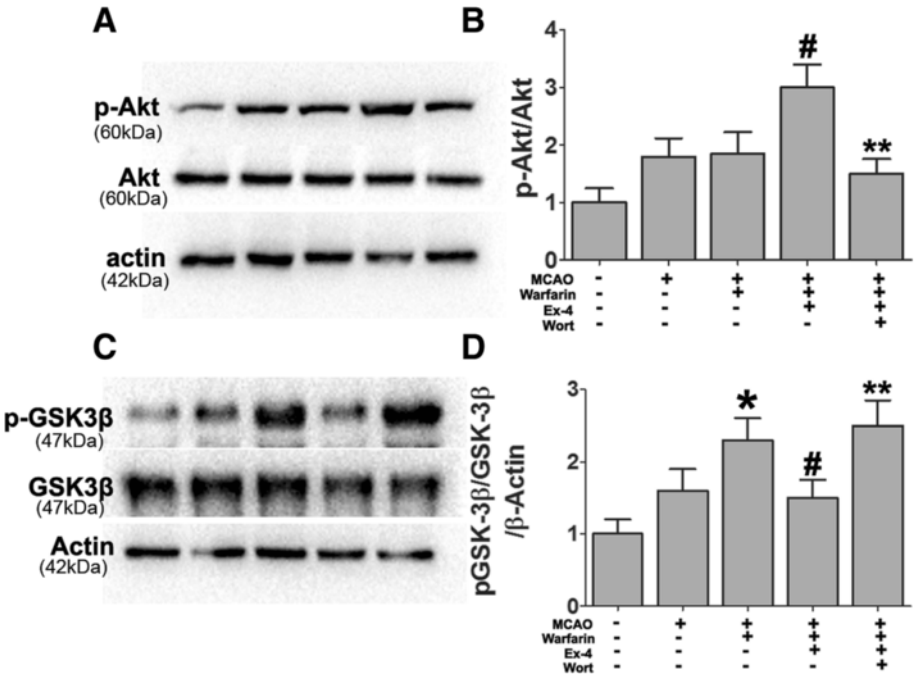

Fig. 4 Effect of Ex-4 on PI3K/Akt/GSK-3β pathway in warfarin-associated HT after cerebral ischemia. Mice were intravenously treated either with Ex-4 (Ex-4, 10 mg/kg) or Ex-4 plus the PI3K inhibitor (wortmannin) (15 μL/kg) right after reperfusion. The expression levels of **a**, **b** p-Akt/Akt and **c**, **d** p-GSK-3β/GSK-3β were analyzed by immunoblotting. Representative blots from six independent experiments with similar results are shown. Data are presented as mean ± SD from six independent experiments and analyzed by one-way ANOVA. *$P < 0.05$ vs. MCAO group; $^{\#}P < 0.05$ vs. MCAO + warfarin group; **$P < 0.05$ vs. MCAO + warfarin + Ex-4 group

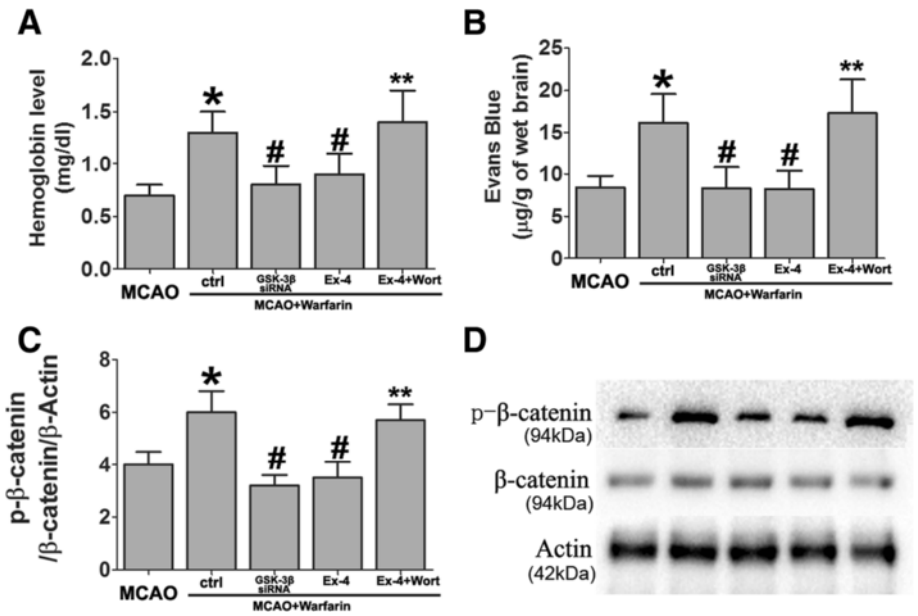

Fig. 5 Ex-4 alleviated warfarin-associated HT after cerebral ischemia through PI3K/Akt/GSK-3β pathway. Effects of GSK-3β siRNA and wortmannin on **a** brain hemoglobin level and **b** Evans blue extravasation were evaluated 72 h after MCAO. **c**, **d** The expression levels of p-β-catenin/β-catenin were also been detected by western blotting. Data are presented as mean ± SD from six independent experiments and analyzed by one-way ANOVA. *$P < 0.05$ vs. MCAO group; $^{\#}P < 0.05$ vs. MCAO + warfarin group; **$P < 0.05$ vs. MCAO + warfarin + Ex-4 group

ischemia. Next, the role of PI3K/Akt/GSK-3β signaling pathway in the integrity of BBB was further investigated using the following antagonists: PI3K inhibitor wortmannin and GSK-3β siRNA in the model of warfarin-associated HT after cerebral ischemia. GSK-3β knockdown by siRNA significantly reduced the warfarin-associated HT. Ex-4 also reversed the warfarin-induced HT in ischemic mice. The mice receiving Ex-4 in combination with wortmannin, however, failed to show this protective effect (Fig. 5a).

Exendin-4 preserves BBB integrity in warfarin-associated intracerebral hemorrhage after cerebral ischemia through PI3K/Akt/GSK-3β pathway

To detect the role of the PI3K/Akt/GSK-3β signaling pathway in preventing BBB disruption in the Ex-4-treated mice, wortmannin and GSK-3β siRNA were used. In the model of warfarin-associated HT after cerebral ischemia, GSK-3β knockdown by siRNA significantly prevented the warfarin-induced BBB disruption. When administered alone, Ex-4 preserved BBB integrity after warfarin-associated HT. Mice receiving Ex-4 in combination with wortmannin failed to demonstrate reduced dye extravasation into the ischemic brain hemisphere (Fig. 5b).

The effect of GSK-3β siRNA on the expression levels of the p-β-catenin/β-catenin ratio was also measured. GSK-3β knockdown by siRNA significantly reduced the expression of p-β-catenin. As shown in Fig. 5c, Ex-4 reduced GSK-3β activation, thereby stabilizing β-catenin. However, when the mice were treated with Ex-4 and wortmannin, this stabilization effect of Ex-4 was completely lost.

The expression levels of tight junction proteins were also detected; warfarin-associated HT reduced claudin-3 and claudin-5 levels. However, Ex-4 treatment significantly increased their expression, and wortmannin reversed the initial increase of claudin-3 and claudin-5 by Ex-4 (Fig. 6a, b).

The PI3K/Akt pathway has been implicated in stabilization of the BBB through decreased expression of

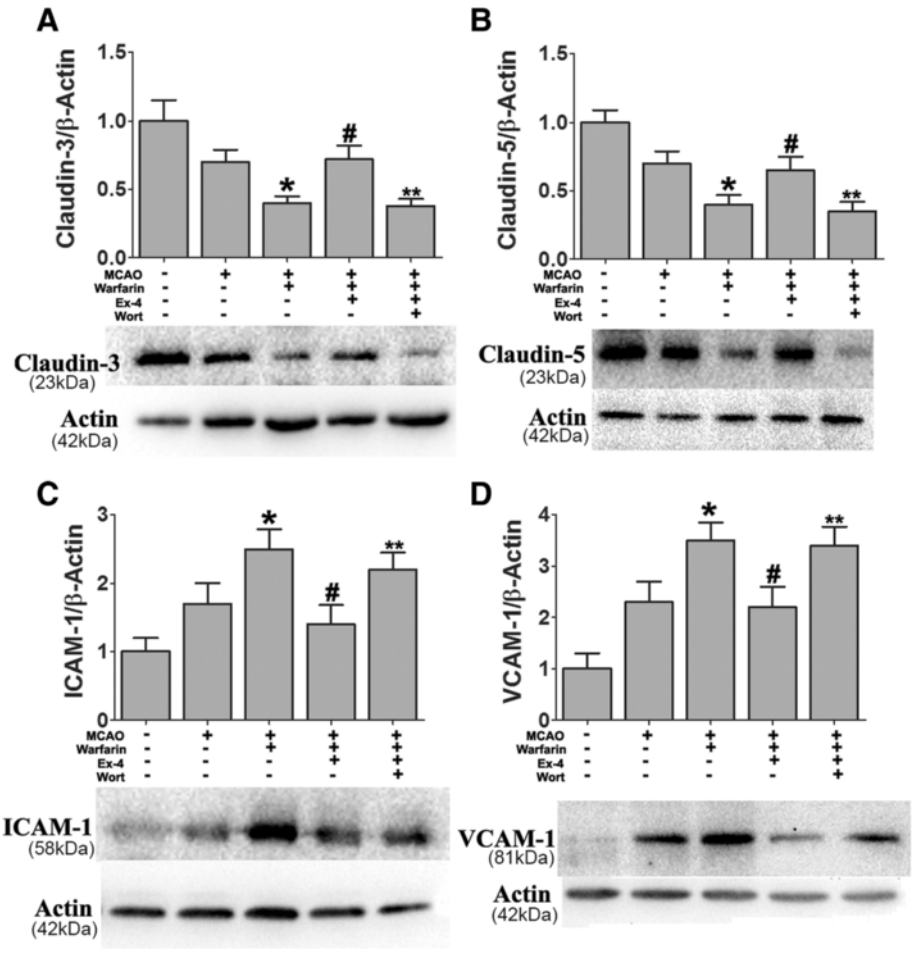

Fig. 6 Ex-4 preserved the BBB integrity after warfarin-associated HT through PI3K/Akt/GSK-3β pathway. Mice were intravenously treated with either Ex-4 (Ex-4, 10 mg/kg) or Ex-4 plus wortmannin (15 μL/kg) right after reperfusion. The expression levels of **a** claudin-3, **b** claudin-5, **c** ICAM-1, and **d** VCAM-1 were analyzed by western blotting. Data are presented as mean ± SD from six independent experiments and analyzed by one-way ANOVA. $^{*}P < 0.05$ vs. MCAO group; $^{\#}P < 0.05$ vs. MCAO + warfarin group; $^{**}P < 0.05$ vs. MCAO + warfarin + Ex-4 group

endothelial adherent proteins vascular cell adhesion molecule-1 (VCAM-1) and interstitial cell adhesion molecule-1 (ICAM-1) [44, 45]. Warfarin-associated HT significantly increased the expression of ICAM-1 and VCAM-1. Both adhesion molecules' expressions were decreased by Ex-4 treatment, and wortmannin reversed the reduction of the adhesion molecules' levels induced by Ex-4 (Fig. 6c, d).

Exendin-4 suppresses oxidative DNA damage and lipid peroxidation in warfarin-associated HT after cerebral ischemia

Next, we investigated whether Ex-4 can control oxidative stress in warfarin-associated HT using lipid peroxidation indicator (HHE) and DNA oxidative injure indicator (8-OHdG). 8-OHdG is a major form of oxidative DNA damage product, and 4-hydroxyhexenal (HHE) is one of the major lipid peroxidation products that are formed by n-3 polyunsaturated fatty acids in cells exposed to oxidative stress [46]. The expression levels of 8-OHdG and HHE were significantly increased in warfarin-associated HT brains compared to MCAO brains. The levels of these oxidative stress markers were significantly decreased in the Ex-4-treated group. When the mice were treated in combination with wortmannin, Ex-4 failed to suppress the expression levels of 8-OHdG and HHE (Fig. 7).

Exendin-4 attenuated pro-inflammatory cytokines in warfarin-associated HT after cerebral ischemia

We additionally examined the role of Ex-4 in modulating neuroinflammation by measuring expression levels of several cytokines such as IKK-β, NF-kB, TNF-α, and IL-1β. The expression levels of IKK-β and NF-kB were significantly increased after warfarin-associated HT compared to MCAO alone, while Ex-4 treatment reduced the effect and wortmannin blocked the reduction induced by Ex-4 (Fig. 8a, b).

The expression levels of TNF-α and IL-1β were evaluated by ELISA. Both these cytokines were upregulated in warfarin-associated HT mice, and Ex-4 blocked the increase concordantly with a similar pattern for IKK-β and NF-kB. The modulating effect of Ex-4 on the cytokines' expression levels were reversed by co-treatment with wortmannin (Fig. 8c, d).

Exendin-4 suppresses neuroinflammation in warfarin-associated HT after cerebral ischemia

Consistent with the changes in cytokine levels, immunofluorescence analysis also showed that warfarin-associated HT robustly enhanced immunofluorescence intensity of Iba1 staining (a marker of microglia/macrophages) in the MCA area compared to the MCAO group (Fig. 9a). The quantification results showed Iba1-positive cells were significantly attenuated in the mice treated with the Ex-4 (Fig. 9b). Further, morphology analysis showed that the number of activated microglia was attenuated in the Ex-4-treated group (Fig. 9e–g). Consistent with these results, double immunofluorescent staining showed Iba1+/TNF-α + cells were elevated in the warfarin-associated HT group and Ex-4 significantly reduced the double positive cells (Additional file 3: Figure S3). Wortmannin blocked this function of Ex-4. Western blotting showed similar results with immunostaining (Fig. 9c). Taken together, these results suggest

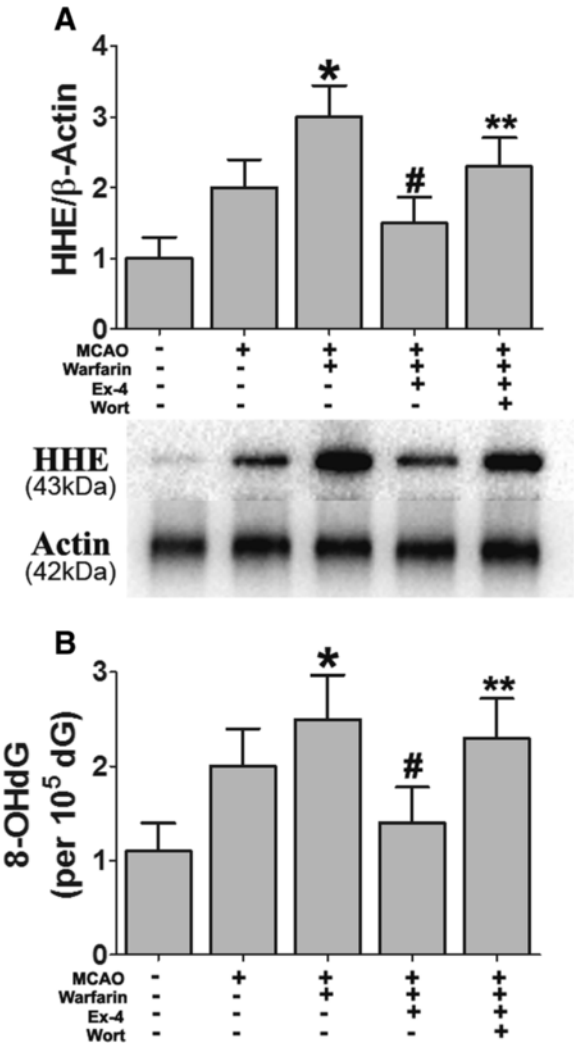

Fig. 7 Ex-4 suppressed oxidative DNA damage and lipid peroxidation in warfarin-associated HT after cerebral ischemia. Mice were intravenously treated with either Ex-4 (Ex-4, 10 mg/kg) or Ex-4 plus wortmannin (15 μL/kg) right after reperfusion. The expression levels of **a** HHE and **b** 8-OHdG in the brain tissue were detected. Data are presented as mean ± SD from six independent experiments and analyzed by one-way ANOVA. $^{*}P < 0.05$ vs. MCAO group; $^{\#}P < 0.05$ vs. MCAO + warfarin group; $^{**}P < 0.05$ vs. MCAO + warfarin + Ex-4 group

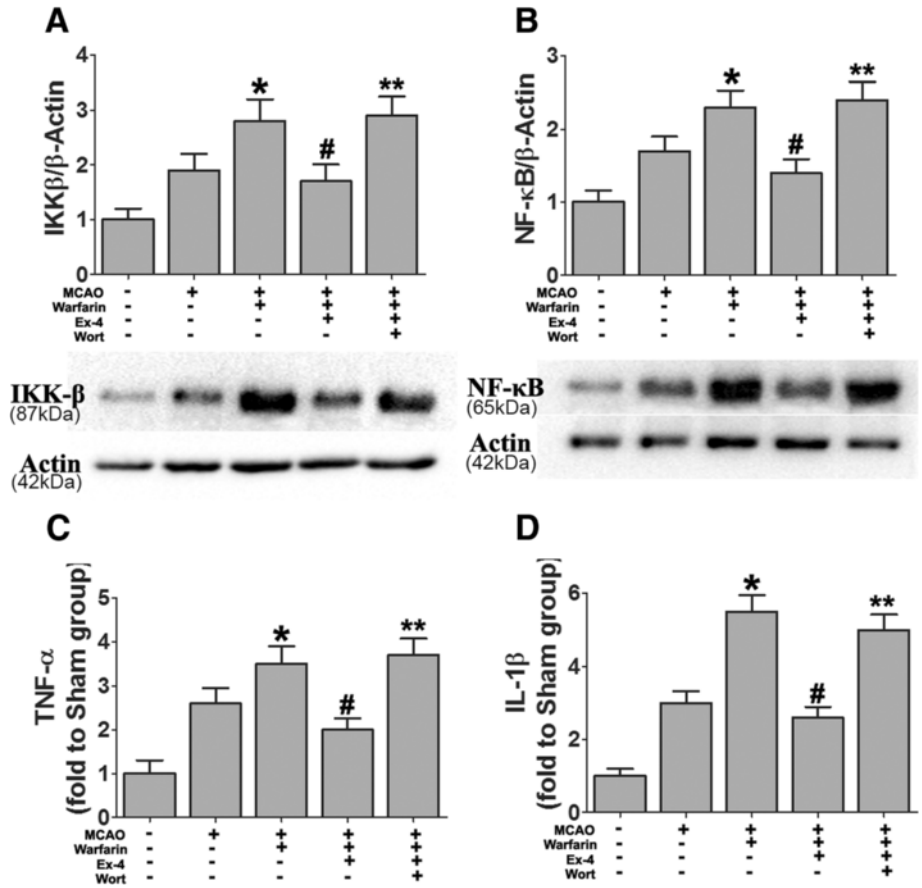

Fig. 8 Ex-4 attenuated pro-inflammatory cytokines in warfarin-associated HT after cerebral ischemia. Mice were intravenously treated with either Ex-4 (Ex-4, 10 mg/kg) or Ex-4 plus wortmannin (15 μL/kg) right after reperfusion. The expression levels of **a** IKK-β and **b** NF-kB were analyzed by western blotting. The concentrations of pro-inflammatory cytokines **c** TNF-α and **d** IL-1β were detected by ELISA. Data are mean ± SD from six independent experiments and analyzed by one-way ANOVA. *$P < 0.05$ vs. MCAO group; #$P < 0.05$ vs. MCAO + warfarin group; **$P < 0.05$ vs. MCAO + warfarin + Ex-4 group

that the protection conferred by Ex-4 was likely mediated by the inhibition on warfarin-associated neuroinflammation after cerebral ischemia.

In addition to brain resident microglia, hematogenous leukocytes have been shown to play a pivotal role in post-stroke neuroinflammation. Among white blood cells, neutrophils have attracted much interest recently and have been intensively studied. The level of myeloperoxidase (MPO) was significantly increased in the warfarin-associated HT group compared to MCAO. Ex-4 treatment reversed the MPO level. The inhibition of Akt by wortmannin restored the MPO level back to that of the warfarin-associated HT group (Fig. 9d).

Discussion

Atrial fibrillation is a severe independent risk factor of stroke, its attributable risk increasing with age up to more than 20 % [47]. INR-driven oral anticoagulation with vitamin K antagonists to an INR of 2–3 reduces the risk of an ischemic stroke by over 60 % and has been the standard of stroke prevention in patients with AF [48]. However, anticoagulation therapy is closely related to HT after ischemia. In addition, cardioembolic stroke also carries with it an increased risk of HT [49]. The chief mechanism of HT is considered to be blood leakage due to disruption of the BBB. Our results showed that pretreatment with warfarin could significantly increase the INR level in a time-dependent manner and dramatically enhance Evans blue leakage provoked by MCAO. Although the infarct volume and neurological deficits were not significantly different between the groups with or without warfarin treatment, warfarin significantly promoted the HT after cerebral ischemia, which is consistent with the permeability measurement results.

GLP-1 and long-acting Ex-4 induce numerous biological actions through the G protein-coupled GLP-1 receptor (GLP-1R). GLP-1R is reportedly expressed in a wide range of tissues, including the brain. Moreover, GLP-1R stimulation has shown neuroprotective actions in previous findings, thereby establishing that GLP-1R

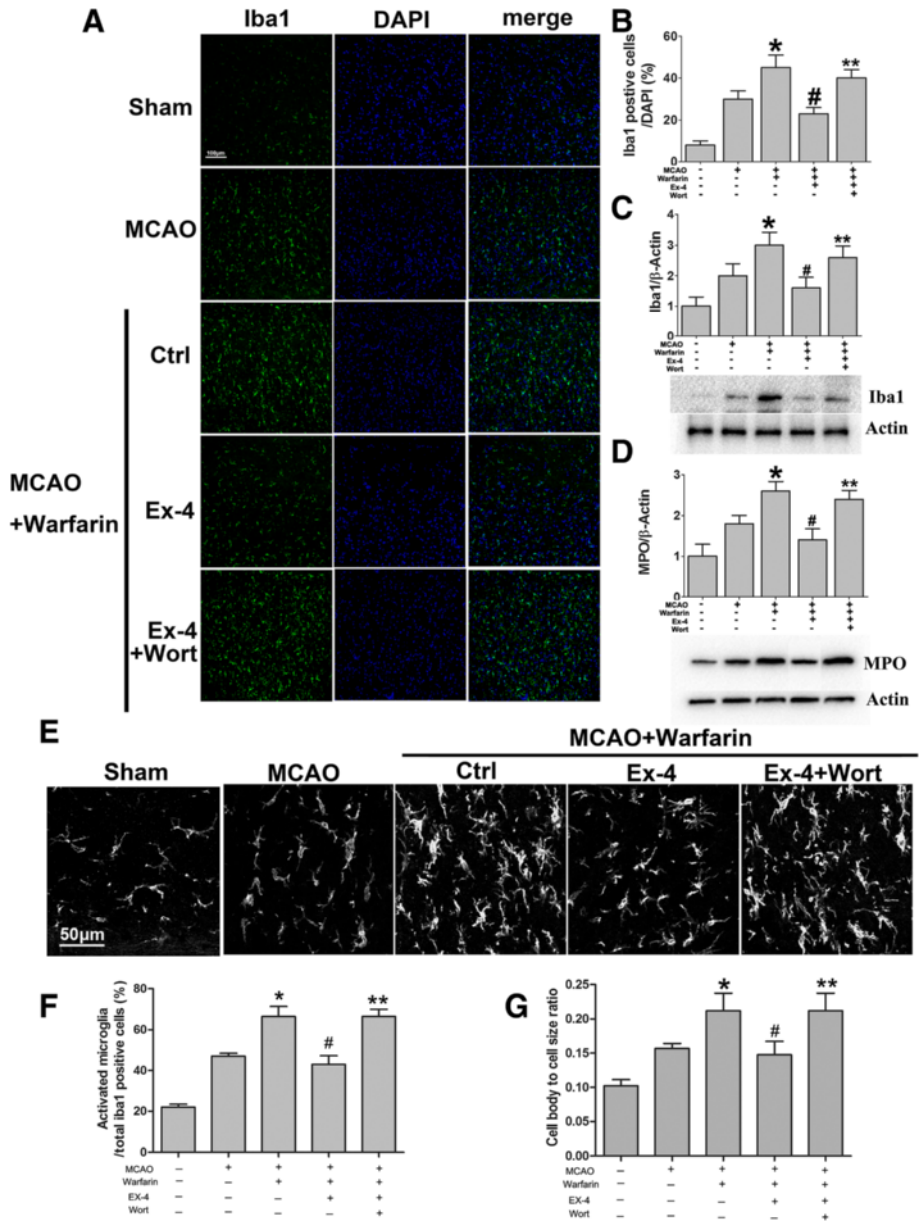

Fig. 9 Ex-4 reduced Iba1+ microglial/macrophage cells and neutrophil infiltration in warfarin-associated HT after cerebral ischemia. Immunostaining of Iba1 was performed in the cortical and subcortical areas supplied by the middle cerebral artery. **a** Representative immunofluorescence images showed Iba1+ (*green*) and DAPI+ (*blue*) microglia/macrophages in the Ex-4-treated mice compared to the warfarin-associated HT group. *Scale bar* 100 μm. **b** Quantitative analysis of Iba1+ cells. The expression levels of Iba1 (**c**) and MPO (**d**) were detected by western blotting. **e** Representative images show microglial morphology in different groups. *Scale bar* 50 μm. **f** The number of activated microglia was expressed as a percentage of the total number of Iba1+ cells. **g** The cell body to cell size ratio of microglia provides additional information about microglial activation. Data are presented as mean ± SD from six independent experiments and analyzed by one-way ANOVA. $^{*}P < 0.05$ vs. MCAO group; $^{\#}P < 0.05$ vs. MCAO + warfarin group; $^{**}P < 0.05$ vs. MCAO + warfarin + Ex-4 group

stimulation protects hippocampal neurons from amyloid-β peptide and glutamate-induced toxicity [50, 51]. As the GLP-1R agonist Ex-4 is permeable to the BBB with a relatively long half time, it has possible clinical applications. Several studies have shown that Ex-4 can protect against oxidative products and neuronal cell death caused by ischemic brain damage [15]. However, to the best of our knowledge, whether GLP-1R stimulation is associated with warfarin-associated HT has not yet been studied. Herein, we reported that Ex-4 prevented the exacerbation of HT caused by warfarin without affecting the infarct volume. The mechanism whereby Ex-4 prevented the

exacerbation of HT might involve maintenance of the expression of tight junction proteins and suppress the neuroinflammation associated with warfarin treatment. The pathways that strengthen the antiapoptotic and neuroprotective effects of Ex-4 after cerebral ischemia mostly converge on activation of the transcription factor cAMP response element-binding protein (CREB) by phosphorylation. In the present study, the PI3K/Akt-GSK-3β signaling pathway appeared to contribute to the protection afforded by Ex-4 in the warfarin-associated HT model.

PI3K/Akt plays a crucial role in the cell death/survival pathway through several different downstream targets including GSK-3β [52]. A temporal increase in phospho-Akt after cerebral ischemia has been reported, and GSK-3β dephosphorylation at tyrosine-216 is accelerated as a downstream target of Akt [53]. The inactivation of GSK-3β via tyrosine-216 dephosphorylation mediates neuronal survival after cerebral ischemia [43]. In addition, the inactivation of GSK-3β results in stabilization of β-catenin, a protein that plays a role in cell adhesion. As a result, free β-catenin is allowed to accumulate and be translocated to the nucleus, binding to the transcription factors to alter target gene expressions [54], such as those of tight junction proteins claudin-3 and claudin-5 [18, 39]. Furthermore, GSK-3β inactivation may also decrease NF-kB expression, thereby reducing neuroinflammation.

In this study, Akt phosphorylation at Ser473 and GSK-3β dephosphorylation at tyr216 were increased in warfarin-associated HT after cerebral ischemia. Administration of Ex-4 substantially decreased HT and maintained the stability of BBB. The reduced dye extravasation and brain hemoglobin level were similar to that achieved by inhibition of GSK-3β. Evidence supporting enhanced BBB stabilization by Ex-4 including decreased adherens (VCAM-1 and ICAM-1) and increased tight junction (claudin-3 and claudin-5) proteins could be totally abolished by wortmannin, a specific PI3K inhibitor. These results suggest that warfarin-associated HT reduced the expression of tight junction proteins. This effect was prevented by treatment with Ex-4 through the PI3K/Akt-GSK-3β pathway. Furthermore, Ex-4 reduced the warfarin-induced hemorrhage volume via a protective effect on vascular endothelial cells.

Inflammation has been recognized as a key contributor to the pathophysiology of cerebral ischemia [55]. Inflammation includes a series of cellular events such as infiltration of neutrophil cells and activation of microglia/macrophages and astrocytes [56]. We found that warfarin-associated HT significantly upregulated Iba1-positive cells. Microglia/macrophage activation, together with elevated expression of pro-inflammatory cytokines such as IKK-β, NF-kB, TNF-α, and IL-1β, demonstrated that the warfarin-associated HT induced a neuroinflammation after cerebral ischemia. It has also been reported that activated microglia/macrophages are major sources of metalloproteinase generation, which is closely associated with ischemia-induced cerebral hemorrhage and edema. NF-kB is a central mediator of these inflammatory processes. Recent evidence has shown that the PI3K/Akt signaling pathway may be an endogenous negative feedback regulator of NF-kB-mediated pro-inflammatory responses [57, 58]. Several pro-inflammatory NF-kB target genes including TNF-α and IL-1β could mediate the deleterious effects on neurons under ischemic conditions. In the present study, we showed that warfarin-induced HT markedly induced the activation of microglia/macrophages and consequently increased the production of pro-inflammatory cytokines and Ex-4 significantly inhibited the neuroinflammation induced by warfarin through the PI3K/Akt-GSK-3β pathway. Moreover, suppression of oxidative damage is also a key factor in neuroprotection. Using 8-OHdG and HHE as markers of oxidative stress, our study showed that Ex-4 reduced the warfarin-induced accumulation of oxidative DNA damage and lipid peroxidation after cerebral ischemia.

Conclusions

Our study results showed that administration of GLP-1 could reduce warfarin-associated HT in mice. This beneficial effect of GLP-1 was associated with attenuating neuroinflammation and BBB disruption by inactivating GSK-3β through the PI3K/Akt pathway. These findings have important clinical implications and would be particularly beneficial in those receiving anticoagulant therapy. Future clinical trials should focus on confirming the efficacy and safety of this therapy.

Additional files

Additional file 1: Figure S1. The PT-INR values after warfarin withdrawal. After warfarin withdrawal, INR values remained stable for the next 6 h and dropped to normal values after 24 h. Data are shown as mean ± SD.

Additional file 2: Figure S2. The rCBF levels in the ischemia and reperfusion stages in MCAO mice. A coated filament was placed on the right middle cerebral artery (MCA) with concurrent recording of laser Doppler cerebral blood flow. In the ischemia stage, the rCBF decreased to <25 % of baseline. After 45 min, the filament was removed and the rCBF increased to 110 % of baseline.

Additional file 3: Figure S3. Representative immunofluorescence images showed co-localization of Iba1 (green) and TNF-α (red) in microglia. Immunostaining of Iba1(green), TNF-α(red), and DAPI (blue) was performed in the cortical and subcortical areas supplied by the middle cerebral artery. (**A**) Representative immunofluorescence images showed the percentage of Iba1+/TNF-α + cells to total Iba1+ cells was increased after warfarin treatment. EX-4 treatment reduced the Iba1+/TNF-α + cells percentage, whereas wortmannin blocked this effect of EX-4. Scale bar 50 μm. (**B**) Quantitative analysis of Iba1 and TNF-α double positive cells/Iba1-positive cells.

Acknowledgements

We are grateful to Baoguo Xiao for his technical support and Min Guo for assisting in preparing this manuscript.

Funding
This study was supported by the National Natural Science Foundation of China 81471173 (to MC) and 81271295 and 81571109 (to QD).

Authors' contributions
MC and QD designed the study. FC and WW performed the experiments, carried out the statistical analysis, and prepared the manuscript. They contributed equally to this work. HD and QY were involved in experiment performance and data collection. MC and QD were responsible for the supervision of the entire project and were involved in the study design, data interpretation, manuscript preparation, and funding. All authors read and approved the final manuscript.

Competing interests
The authors declare that they have no competing interests.

Consent for publication
Not applicable.

Ethics approval and consent to participate
The study was approved by the Ethics Committee of Fudan University, Shanghai, China. The approval number from IRB is "20150572A259."

Author details
[1]Department of Neurology, Huashan Hospital, State Key Laboratory of Medical Neurobiology, Fudan University, No. 12 Middle Wulumuqi Road, Shanghai 200040, China. [2]The Department of Clinical Laboratory, Central Laboratory, Jing'an District Centre Hospital of Shanghai, Huashan Hospital Fudan University Jing'an Branch, No. 259 Xi Kang Road, Shanghai 200040, China.

Received: 29 December 2015 Accepted: 14 July 2016
Published online: 26 August 2016

References

1. Lopez AD, Mathers CD, Ezzati M, Jamison DT, Murray CJ. Global and regional burden of disease and risk factors, 2001: systematic analysis of population health data. Lancet. 2006;367:1747–57.
2. Go AS, Hylek EM, Phillips KA, Chang Y, Henault LE, Selby JV, Singer DE. Prevalence of diagnosed atrial fibrillation in adults: national implications for rhythm management and stroke prevention: the anticoagulation and risk factors in atrial fibrillation (ATRIA) Study. JAMA. 2001;285:2370–5.
3. Go AS. The epidemiology of atrial fibrillation in elderly persons: the tip of the iceberg. Am J Geriatr Cardiol. 2005;14:56–61.
4. Kucher N, Castellanos LR, Quiroz R, Koo S, Fanikos J, Goldhaber SZ. Time trends in warfarin-associated hemorrhage. Am J Cardiol. 2004;94:403–6.
5. Steiner T, Rosand J, Diringer M. Intracerebral hemorrhage associated with oral anticoagulant therapy: current practices and unresolved questions. Stroke. 2006;37:256–62.
6. Flaherty ML, Kissela B, Woo D, Kleindorfer D, Alwell K, Sekar P, Moomaw CJ, Haverbusch M, Broderick JP. The increasing incidence of anticoagulant-associated intracerebral hemorrhage. Neurology. 2007;68:116–21.
7. Alexandrov AV, Black SE, Ehrlich LE, Caldwell CB, Norris JW. Predictors of hemorrhagic transformation occurring spontaneously and on anticoagulants in patients with acute ischemic stroke. Stroke. 1997;28:1198–202.
8. Pfeilschifter W, Spitzer D, Czech-Zechmeister B, Steinmetz H, Foerch C. Increased risk of hemorrhagic transformation in ischemic stroke occurring during warfarin anticoagulation: an experimental study in mice. Stroke. 2011;42:1116–21.
9. Jickling GC, Liu D, Stamova B, Ander BP, Zhan X, Lu A, Sharp FR. Hemorrhagic transformation after ischemic stroke in animals and humans. J Cereb Blood Flow Metab. 2014;34:185–99.
10. Knight RA, Barker PB, Fagan SC, Li Y, Jacobs MA, Welch KM. Prediction of impending hemorrhagic transformation in ischemic stroke using magnetic resonance imaging in rats. Stroke. 1998;29:144–51.
11. Ozkul-Wermester O, Guegan-Massardier E, Triquenot A, Borden A, Perot G, Gerardin E. Increased blood–brain barrier permeability on perfusion computed tomography predicts hemorrhagic transformation in acute ischemic stroke. Eur Neurol. 2014;72:45–53.
12. Khatri R, McKinney AM, Swenson B, Janardhan V. Blood–brain barrier, reperfusion injury, and hemorrhagic transformation in acute ischemic stroke. Neurology. 2012;79:S52–7.
13. Baggio LL, Drucker DJ. Biology of incretins: GLP-1 and GIP. Gastroenterology. 2007;132:2131–57.
14. Zhang H, Meng J, Li X, Zhou S, Qu D, Wang N, Jia M, Ma X, Luo X. Pro-GLP-1, a Pro-drug of GLP-1, is neuroprotective in cerebral ischemia. Eur J Pharm Sci. 2015;70:82–91.
15. Teramoto S, Miyamoto N, Yatomi K, Tanaka Y, Oishi H, Arai H, Hattori N, Urabe T. Exendin-4, a glucagon-like peptide-1 receptor agonist, provides neuroprotection in mice transient focal cerebral ischemia. J Cereb Blood Flow Metab. 2011;31:1696–705.
16. Guturi KK, Mandal T, Chatterjee A, Sarkar M, Bhattacharya S, Chatterjee U, Ghosh MK. Mechanism of beta-catenin-mediated transcriptional regulation of epidermal growth factor receptor expression in glycogen synthase kinase 3 beta-inactivated prostate cancer cells. J Biol Chem. 2012;287:18287–96.
17. Wang WC, Tsai JJ, Kuo CY, Chen HM, Kao SH. Non-proteolytic house dust mite allergen, Der p 2, upregulated expression of tight junction molecule claudin-2 associated with Akt/GSK-3beta/beta-catenin signaling pathway. J Cell Biochem. 2011;112:1544–51.
18. Liebner S, Corada M, Bangsow T, Babbage J, Taddei A, Czupalla CJ, Reis M, Felici A, Wolburg H, Fruttiger M, et al. Wnt/beta-catenin signaling controls development of the blood–brain barrier. J Cell Biol. 2008;183:409–17.
19. Krafft PR, Altay O, Rolland WB, Duris K, Lekic T, Tang J, Zhang JH. alpha7 nicotinic acetylcholine receptor agonism confers neuroprotection through GSK-3beta inhibition in a mouse model of intracerebral hemorrhage. Stroke. 2012;43:844–50.
20. Linseman DA, Butts BD, Precht TA, Phelps RA, Le SS, Laessig TA, Bouchard RJ, Florez-McClure ML, Heidenreich KA. Glycogen synthase kinase-3beta phosphorylates Bax and promotes its mitochondrial localization during neuronal apoptosis. J Neurosci. 2004;24:9993–10002.
21. Zhao R, Zhang Z, Song Y, Wang D, Qi J, Wen S. Implication of phosphatidylinositol-3 kinase/Akt/glycogen synthase kinase-3beta pathway in ginsenoside Rb1's attenuation of beta-amyloid-induced neurotoxicity and tau phosphorylation. J Ethnopharmacol. 2011;133:1109–16.
22. Maixner DW, Weng HR. The Role of Glycogen Synthase Kinase 3 Beta in Neuroinflammation and Pain. J Pharm Pharmacol (Los Angel). 2013;1:001.
23. Morales-Garcia JA, Susin C, Alonso-Gil S, Perez DI, Palomo V, Perez C, Conde S, Santos A, Gil C, Martinez A, Perez-Castillo A. Glycogen synthase kinase-3 inhibitors as potent therapeutic agents for the treatment of Parkinson disease. ACS Chem Neurosci. 2013;4:350–60.
24. Phiel CJ, Wilson CA, Lee VM, Klein PS. GSK-3alpha regulates production of Alzheimer's disease amyloid-beta peptides. Nature. 2003;423:435–9.
25. Foerch C, Arai K, Jin G, Park KP, Pallast S, van Leyen K, Lo EH. Experimental model of warfarin-associated intracerebral hemorrhage. Stroke. 2008;39:3397–404.
26. Kitashoji A, Egashira Y, Mishiro K, Suzuki Y, Ito H, Tsuruma K, Shimazawa M, Hara H. Cilostazol ameliorates warfarin-induced hemorrhagic transformation after cerebral ischemia in mice. Stroke. 2013;44:2862–8.
27. Lin TN, He YY, Wu G, Khan M, Hsu CY. Effect of brain edema on infarct volume in a focal cerebral ischemia model in rats. Stroke. 1993;24:117–21.
28. Li X, Blizzard KK, Zeng Z, DeVries AC, Hurn PD, McCullough LD. Chronic behavioral testing after focal ischemia in the mouse: functional recovery and the effects of gender. Exp Neurol. 2004;187:94–104.
29. Doeppner TR, Kaltwasser B, Bahr M, Hermann DM. Effects of neural progenitor cells on post-stroke neurological impairment-a detailed and comprehensive analysis of behavioral tests. Front Cell Neurosci. 2014;8:338.
30. Li L, McBride DW, Doycheva D, Dixon BJ, Krafft PR, Zhang JH, Tang J. G-CSF attenuates neuroinflammation and stabilizes the blood–brain barrier via the PI3K/Akt/GSK-3beta signaling pathway following neonatal hypoxia-ischemia in rats. Exp Neurol. 2015.
31. Souza DG, Pinho V, Pesquero JL, Lomez ES, Poole S, Juliano L, Correa Jr A, de A Castro MS, Teixeira MM, de Castro MS, Teixeira MM. Role of the bradykinin B2 receptor for the local and systemic inflammatory response that follows severe reperfusion injury. Br J Pharmacol. 2003;139:129–39.
32. Piao F, Ma N, Hiraku Y, Murata M, Oikawa S, Cheng F, Zhong L, Yamauchi T, Kawanishi S, Yokoyama K. Oxidative DNA damage in relation to neurotoxicity in the brain of mice exposed to arsenic at environmentally relevant levels. J Occup Health. 2005;47:445–9.

33. Lemiere S, Cossu-Leguille C, Charissou AM, Vasseur P. DNA damage (comet assay) and 8-oxodGuo (HPLC-EC) in relation to oxidative stress in the freshwater bivalve Unio tumidus. Biomarkers. 2005;10:41–57.
34. Soltys Z, Ziaja M, Pawlinski R, Setkowicz Z, Janeczko K. Morphology of reactive microglia in the injured cerebral cortex. Fractal analysis and complementary quantitative methods. J Neurosci Res. 2001;63:90–7.
35. Monif M, Reid CA, Powell KL, Drummond KJ, O'Brien TJ, Williams DA. Interleukin-1beta has trophic effects in microglia and its release is mediated by P2X7R pore. J Neuroinflammation. 2016;13:173.
36. Hovens I, Nyakas C, Schoemaker R. A novel method for evaluating microglial activation using ionized calcium-binding adaptor protein-1 staining: cell body to cell size ratio. Neuroimmunol Neuroinflammation. 2014;1:82.
37. Rossa J, Ploeger C, Vorreiter F, Saleh T, Protze J, Gunzel D, Wolburg H, Krause G, Piontek J. Claudin-3 and claudin-5 protein folding and assembly into the tight junction are controlled by non-conserved residues in the transmembrane 3 (TM3) and extracellular loop 2 (ECL2) segments. J Biol Chem. 2014;289:7641–53.
38. Jiao H, Wang Z, Liu Y, Wang P, Xue Y. Specific role of tight junction proteins claudin-5, occludin, and ZO-1 of the blood–brain barrier in a focal cerebral ischemic insult. J Mol Neurosci. 2011;44:130–9.
39. Taddei A, Giampietro C, Conti A, Orsenigo F, Breviario F, Pirazzoli V, Potente M, Daly C, Dimmeler S, Dejana E. Endothelial adherens junctions control tight junctions by VE-cadherin-mediated upregulation of claudin-5. Nat Cell Biol. 2008;10:923–34.
40. Elyaman W, Yardin C, Hugon J. Involvement of glycogen synthase kinase-3beta and tau phosphorylation in neuronal Golgi disassembly. J Neurochem. 2002;81:870–80.
41. Leis H, Segrelles C, Ruiz S, Santos M, Paramio JM. Expression, localization, and activity of glycogen synthase kinase 3beta during mouse skin tumorigenesis. Mol Carcinog. 2002;35:180–5.
42. Ramirez SH, Fan S, Dykstra H, Rom S, Mercer A, Reichenbach NL, Gofman L, Persidsky Y. Inhibition of glycogen synthase kinase 3beta promotes tight junction stability in brain endothelial cells by half-life extension of occludin and claudin-5. PLoS One. 2013;8, e55972.
43. Krafft PR, Caner B, Klebe D, Rolland WB, Tang J, Zhang JH. PHA-543613 preserves blood–brain barrier integrity after intracerebral hemorrhage in mice. Stroke. 2013;44:1743–7.
44. Tsoyi K, Jang HJ, Nizamutdinova IT, Park K, Kim YM, Kim HJ, Seo HG, Lee JH, Chang KC. PTEN differentially regulates expressions of ICAM-1 and VCAM-1 through PI3K/Akt/GSK-3beta/GATA-6 signaling pathways in TNF-alpha-activated human endothelial cells. Atherosclerosis. 2010;213:115–21.
45. Tsoyi K, Kim WS, Kim YM, Kim HJ, Seo HG, Lee JH, Yun-Choi HS, Chang KC. Upregulation of PTEN by CKD712, a synthetic tetrahydroisoquinoline alkaloid, selectively inhibits lipopolysaccharide-induced VCAM-1 but not ICAM-1 expression in human endothelial cells. Atherosclerosis. 2009;207:412–9.
46. Yamada S, Funada T, Shibata N, Kobayashi M, Kawai Y, Tatsuda E, Furuhata A, Uchida K. Protein-bound 4-hydroxy-2-hexenal as a marker of oxidized n-3 polyunsaturated fatty acids. J Lipid Res. 2004;45:626–34.
47. Wolf PA, Abbott RD, Kannel WB. Atrial fibrillation as an independent risk factor for stroke: the Framingham Study. Stroke. 1991;22:983–8.
48. Hart RG, Pearce LA, Aguilar MI. Meta-analysis: antithrombotic therapy to prevent stroke in patients who have nonvalvular atrial fibrillation. Ann Intern Med. 2007;146:857–67.
49. Kelley RE, Berger JR, Alter M, Kovacs AG. Cerebral ischemia and atrial fibrillation: prospective study. Neurology. 1984;34:1285–91.
50. Perry T, Lahiri DK, Sambamurti K, Chen D, Mattson MP, Egan JM, Greig NH. Glucagon-like peptide-1 decreases endogenous amyloid-beta peptide (Abeta) levels and protects hippocampal neurons from death induced by Abeta and iron. J Neurosci Res. 2003;72:603–12.
51. During MJ, Cao L, Zuzga DS, Francis JS, Fitzsimons HL, Jiao X, Bland RJ, Klugmann M, Banks WA, Drucker DJ, Haile CN. Glucagon-like peptide-1 receptor is involved in learning and neuroprotection. Nat Med. 2003;9:1173–9.
52. Cross DA, Alessi DR, Cohen P, Andjelkovich M, Hemmings BA. Inhibition of glycogen synthase kinase-3 by insulin mediated by protein kinase B. Nature. 1995;378:785–9.
53. Noshita N, Lewen A, Sugawara T, Chan PH. Evidence of phosphorylation of Akt and neuronal survival after transient focal cerebral ischemia in mice. J Cereb Blood Flow Metab. 2001;21:1442–50.
54. Lim JC, Kania KD, Wijesuriya H, Chawla S, Sethi JK, Pulaski L, Romero IA, Couraud PO, Weksler BB, Hladky SB, Barrand MA. Activation of beta-catenin signalling by GSK-3 inhibition increases p-glycoprotein expression in brain endothelial cells. J Neurochem. 2008;106:1855–65.
55. Iadecola C, Anrather J. The immunology of stroke: from mechanisms to translation. Nat Med. 2011;17:796–808.
56. Muir KW, Tyrrell P, Sattar N, Warburton E. Inflammation and ischaemic stroke. Curr Opin Neurol. 2007;20:334–42.
57. Fukao T, Koyasu S. PI3K and negative regulation of TLR signaling. Trends Immunol. 2003;24:358–63.
58. Broughton BR, Reutens DC, Sobey CG. Apoptotic mechanisms after cerebral ischemia. Stroke. 2009;40:e331–9.